

Stress Analysis Method for a Clearance-Fit Bolt Under Bearing Loads

R. A. Naik* and J. H. Crews Jr.†
NASA Langley Research Center, Hampton, Virginia

Mechanically fastened joints are becoming widely used in composite aerospace structures. In most such applications, some bolt-hole clearance exists which may influence the stresses around the hole. In the past, analyses of a clearance-fit bolt have involved complicated iterative-incremental schemes or simplifying assumptions for the stresses or displacements in the contact region. A simple method of analysis has been developed and verified in the present study. It uses an inverse formulation with a finite element analysis. Conditions along the bolt-hole contact arc are specified by displacement constraint equations. The present method is simple to apply and can be implemented with most general-purpose finite element programs. The method was applied to analyze a single-fastener, clearance-fit joint with typical values of clearance. In this analysis, a rigid, frictionless bolt was used with a quasi-isotropic graphite/epoxy laminate. Results showed that the contact arc as well as the peak stresses around the hole and their locations were strongly influenced by the clearance. After a slight initial nonlinearity, the peak stresses varied linearly with applied load. The typical clearance levels were shown to have only a minor influence on the overall joint stiffness.

Nomenclature

c	= radial bolt-hole clearance, m
c_d	= diametrical bolt-hole clearance, %
d	= hole diameter, m
e	= edge distance, m
L_t	= tension length, m
P	= applied load, N
r, θ	= polar coordinates, m, degrees
r_b	= bolt radius, m
R	= hole radius, m
S_b, S_b^*	= nominal bearing stress, MPa
t	= plate thickness, m
u, v	= x and y displacements, m
w	= plate width, m
x, y	= Cartesian coordinates, m
θ_c	= bolt-hole contact angle, degrees
σ	= stress component, MPa
σ_{rr}	= radial stress component, MPa
$\sigma_{\theta\theta}$	= tangential stress component, MPa

Introduction

MECHANICALLY fastened joints are commonly used in aerospace structures. To better understand the complex behavior of such joints, it is important to develop accurate stress analyses for bearing-loaded fastener holes. This is especially important for composite structures since they can be seriously weakened by fastener holes and often have rather complex failure modes. Furthermore, in most joints some clearance exists between the fastener and the hole. This clearance is difficult to account for in a stress analysis because it leads to a contact region at the bolt-hole interface that increases nonlinearly with the bearing load.

In 1970, Harris et al.¹ studied the influence of clearance in mechanically fastened joints. In their analysis of the nonlinear contact at the bolt-hole interface, they used a trial and error procedure to determine the redundant radial reactions between the plate and the fastener for a given load level. Several studies have since used numerical techniques to investigate the nonlinear contact problem associated with a smooth clearance-fit bolt under bearing loads.²⁻⁵ Oplinger and Gandhi² used an analytical function approach in conjunction with least squares boundary collocation. Waszczak and Cruse³ introduced a finite element approach, but replaced the bolt with an assumed cosine stress distribution. Eshwar⁴ developed a continuum analysis together with an inverse technique in which the extent of interface contact was specified and the bearing load was calculated. Mangalgi et al.⁵ also used an inverse technique but with a finite element analysis and an assumed cosine distribution of radial displacements at the bolt-hole interface. Several studies have also been done⁶⁻⁹ for the more general problem of the contact between elastic bodies including the effects of clearance. These procedures could also be used in the analysis of clearance-fit bearing-loaded holes. Francavilla and Zienkiewicz⁶ used an iterative finite element formulation in terms of the contact pressures at possible contact points of the two bodies. White and Enderby⁷ also used a finite element approach but with special elements at possible contact points and an iterative scheme. Sholes and Strover⁸ employed an incremental piecewise-linear finite element analysis. Chan and Tuba⁹ introduced an iterative finite element procedure to include the effects of both clearance and friction. A comprehensive review of elastic analyses of pin joints has been done by Rao¹⁰ in 1978. More recently, Wilkinson, et al.¹¹ used an iterative-incremental finite element scheme that accounted for friction and clearance. Kim¹² determined bolt contact angles using a combined photoelastic-finite-element method and an interactive computer graphics method. All of these numerical analyses used an iterative-incremental approach or made simplifying assumptions for the stresses or displacements in the contact region.

In the present study a simple numerical technique was developed for the stress analysis of a clearance-fit bolt under bearing loads. The technique uses a finite element analysis with an inverse formulation like that in Ref. 5. Conditions along the bolt-hole interface are specified by constraint equa-

Received Feb. 25, 1985; presented as Paper 85-0746 at the AIAA/ASME/AHS 26th Structures, Structural Dynamics and Materials Conference, Orlando, FL, April 15-17, 1985; revision received Nov. 15, 1985. This paper is declared a work of the U.S. Government and is not subject to copyright protection in the United States.

*Graduate Student, Old Dominion University, Norfolk, VA. Student Member AIAA.

†Senior Engineer, Materials Division.

tions. These equations describe the contact conditions more realistically than the distributions usually assumed for radial displacement or stress. Furthermore, the present technique does not need an iterative-incremental method of solution. A single-fastener clearance-fit joint was analyzed for a typical range of clearance found in aerospace applications. The finite element analysis was performed using the NASTRAN computer code. The material properties used in the analysis represented a quasi-isotropic T300/5208 graphite/epoxy laminate. The bolt was assumed to be rigid and the interface to be frictionless.

Results are presented as curves relating the applied bearing stress and the bolt-hole contact angle. First, results are compared with solutions from the literature to evaluate the present approach. Next, results are presented to show the influence of clearance on the interface contact angle and the local stress distributions along the hole boundary. Finally, the peak local stresses, hole elongations, and overall plate deformations are plotted for a range of bearing loads using typical clearance values.

Analysis

The configuration and loading analyzed in the present study are shown in Fig. 1. The bolt-bearing load results in a nominal bearing stress S_b at the hole and is reacted in tension at the left end of the model. The configuration is described by the tension length L_t , the edge distance e , the width w , and the hole diameter d . The diametrical clearance c_d between the hole and the bolt is expressed as a percentage of d . For the snug-fit joint ($c_d=0$), the contact angle θ_c along the bolt-hole interface, does not change with S_b and a simple linear stress analysis can be used. However, for the clearance-fit joint ($c_d>0$), the contact angle θ_c increases nonlinearly with S_b as shown in Fig. 2. This nonlinearly varying boundary condition at the bolt-hole interface greatly complicates the stress analysis.

Inverse Formulation

An iterative-incremental method could be used to determine the contact angle θ_c for a given nominal bearing stress S_b or an inverse technique can be used to determine the nominal bearing stress S_b for a given contact angle θ_c . The inverse technique is simpler to use because the boundary conditions are fixed and are known at the outset. Therefore, the inverse technique, with a finite element analysis, was used in the present work. Although the contact problem is nonlinear, the inverse technique requires only linear finite element analyses to arrive at a solution; thus, linear NASTRAN procedures were used to solve this nonlinear problem. As previously mentioned, the conditions along the bolt-hole interface were specified by displacement constraint equations. The formulation of these constraint equations and the solution procedure are described in the following two sections.

Displacement Constraint Equations

Figure 3 shows the analysis model, where the bolt radius r_b is smaller than the hole radius R by the amount of radial clearance c . When no load is applied, the only contact point between the bolt and the hole is at point A. To simplify the analysis, the bolt is assumed to be fixed in space. The origin of the reference coordinate system is located at the center of the undeformed hole. After the model is loaded, points along the hole boundary which lie within an assumed contact arc AB have moved to the frictionless surface of the fixed rigid bolt.

Consider a point $P(x,y)$ on the hole boundary within the assumed contact arc AB (see Fig. 3). Let u and v be the x - and y -displacements necessary to move point P from its original position to a point on the surface of the bolt. The deformed position of P may be described by the following

equation:

$$[(x-c)+u]^2 + [y+v]^2 = r_b^2 \quad (1)$$

By expressing x and y in polar coordinates and neglecting the higher order terms in u and v , Eq. (1) may be rewritten as follows:

$$Au + Bv = C \quad (2)$$

where

$$A = R \cos \theta - c \quad (3)$$

$$B = R \sin \theta \quad (4)$$

and

$$C = (\frac{1}{2})(r_b^2 - R^2) + cR \cos \theta - (\frac{1}{2})c^2 \quad (5)$$

Equation (2) is a constraint equation for the u - and v -displacements of any point, $P(x,y)$ on the contact arc AB. For any point within the assumed θ_c , the quantities A , B ,

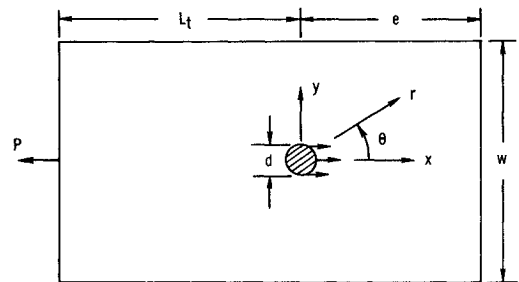


Fig. 1 Configuration and loading.

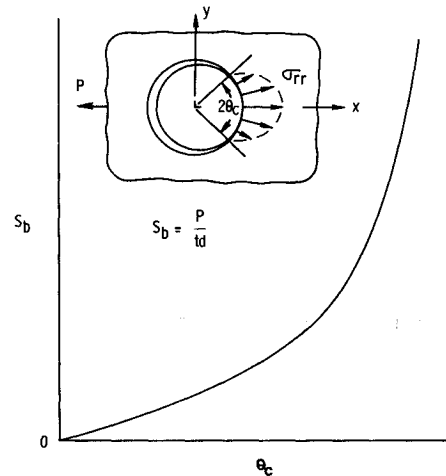


Fig. 2 Nonlinear relationship between bearing stress and contact angle.

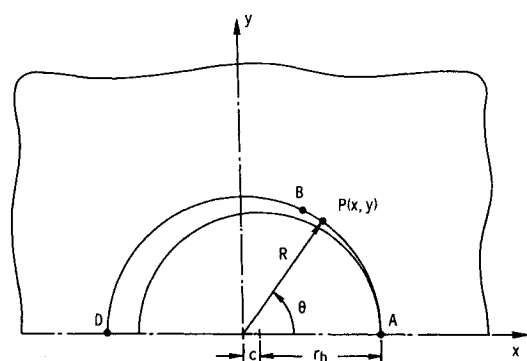


Fig. 3 Hole clearance notation.

and C can be computed at the outset since they are functions of the initial geometry. In the finite element analysis, the displacements of each node within the contact region can be specified by applying Eq. (2) as a multi-point constraint. Note that the region beyond the contact arc on the hole boundary is stress free. This fact will be used later in the analysis.

Solution Procedure

To determine the correct nominal bearing stress for the assumed contact angle, a simple procedure using a finite element analysis was established. Figure 4 shows the mesh used for the finite element analysis. One-half of the plate was modeled by isoparametric elements. Nodes were placed at every 0.9375° along the hole boundary. At node A , which was assumed to be in contact with the rigid bolt throughout the analysis, all degrees of freedom were set equal to zero. For an assumed contact angle θ_c , displacements of the nodes within the contact arc were restricted to those allowed by the multi-point constraints given by Eq. (2). Thus all the boundary conditions, including those along the bolt-hole interface, are known at the outset. However, since the contact angle θ_c and the nominal bearing stress S_b are nonlinearly related, the correct S_b corresponding to the assumed θ_c is still unknown.

The correct S_b level for the assumed θ_c value was determined by a simple procedure.⁵ Note that for a specified θ_c , the problem is linear and thus, the stresses in the plate are linearly related to S_b . A linear equation relating σ_{rr} and S_b can be written as

$$\sigma_{rr}(r, \theta) = F_1(r, \theta)S_b + F_2(r, \theta) \quad (6)$$

The first term in this equation represents the σ_{rr} component solely attributable to the applied bearing load. The second term represents the σ_{rr} associated with the imposed multi-point constraints. This second term is a function of clearance, as indicated by Eq. (2).

As mentioned earlier, the hole boundary region beyond the contact arc is stress free. Thus,

$$\sigma_{rr}(R, \theta) = 0 \quad \theta_c \leq \theta \leq \pi \quad (7)$$

This stress boundary condition was imposed at the end of the contact arc as

$$\sigma_{rr}(R, \theta_c) = 0 \quad (8)$$

The correct solution must satisfy Eq. (8). If S_b^* is the correct nominal bearing stress corresponding to the contact angle θ_c then, from Eqs. (6) and (8), we have the following

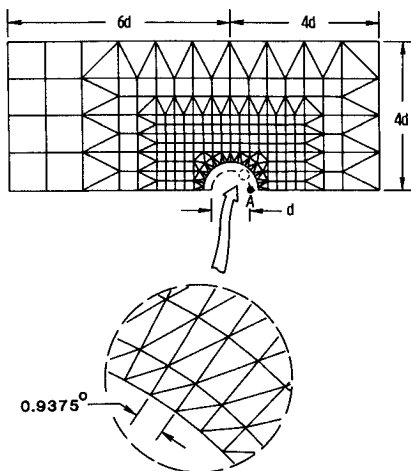


Fig. 4 Finite element model.

relation:

$$F_1(R, \theta_c)S_b^* + F_2(R, \theta_c) = 0 \quad (9)$$

This equation can be rewritten as follows:

$$S_b^* = -F_2(R, \theta_c)/F_1(R, \theta_c) \quad (10)$$

Equation (10) was evaluated by the following procedure. For an assumed θ_c , an S_b was selected arbitrarily and the σ_{rr} was calculated at the end of the contact arc using a finite-element analysis. These S_b and σ_{rr} values were then substituted into Eq. (6) to get an equation for $F_1(R, \theta_c)$ and $F_2(R, \theta_c)$. Next, a second S_b was selected and again the corresponding σ_{rr} at the end of the contact was calculated. This second set of S_b and σ_{rr} values was used with Eq. (6) to get a second equation for $F_1(R, \theta_c)$ and $F_2(R, \theta_c)$. The two equations were solved to determine $F_1(R, \theta_c)$ and $F_2(R, \theta_c)$ which were used in Eq. (10) to find S_b^* . This procedure was repeated for a series of θ_c values to determine the corresponding S_b^* values. These pairs of θ_c and S_b^* values were then plotted as $S_b - \theta_c$ curves for the nonlinear contact in the clearance-fit joint.

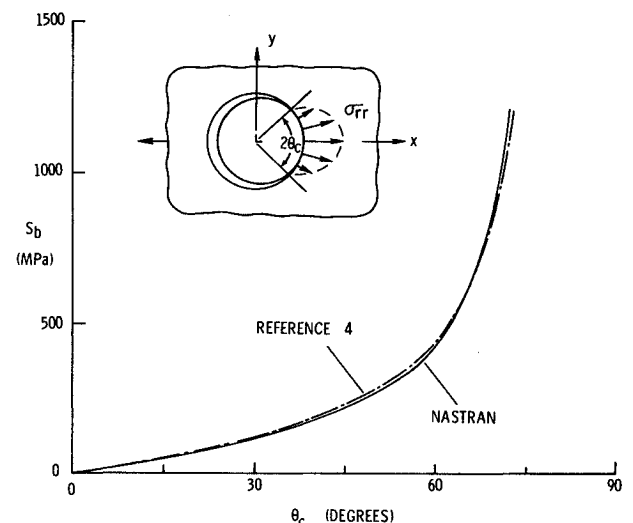


Fig. 5 Comparison of infinite plate results.

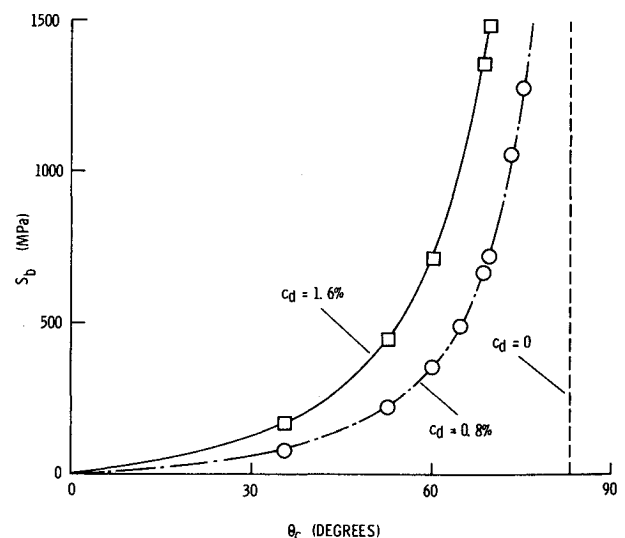


Fig. 6 Effect of clearance on the $S_b - \theta_c$ relationship.

Results and Discussion

First, to evaluate the accuracy of the present analysis, results are compared with previously published work for the case of an infinite, isotropic plate. Next, the effects of clearance on the contact angle, local stresses, and hole elongation are presented. Also, the effect of different levels of the nominal bearing stress on the local stress distribution is shown.

The $S_b - \theta_c$ curve obtained for an essentially infinite plate ($w = 20d$, $e = 10d$, $L_t = 10d$) with isotropic material properties using the NASTRAN program is shown as a solid line in Fig. 5. The dash-dot curve represents the infinite plate results obtained by Eshwar⁴ using a continuum analysis. For both curves, the diametrical clearance c_d was 0.8%. The two curves are in excellent agreement, which verifies the finite element model and the numerical procedure used in the present study.

Two values of the bolt-hole clearance, $c_d = 0.8\%$ and 1.6% , were used in the present study. These values are typical of clearances recommended for mechanically fastened joints in aerospace structures made of composite materials.¹³ In addition, the snug-fit case ($c_d = 0$) was used as a reference. All of the following results were obtained for the finite size plate shown in Fig. 4 with $w = 8d$, $e = 4d$, $L_t = 6d$. The influence of the value of c_d on the $S_b - \theta_c$ curves is shown in Fig. 6. The dashed line corresponds to the snug-fit case ($c_d = 0$). In this linear case, the contact angle, $\theta_c = 83$ deg, does not change with increasing S_b . For both the nonlinear cases (the dashed-dot and solid curves), at low levels of S_b , the contact angle, θ_c , increased rapidly for small increases in S_b . At higher S_b levels, the contact angle was less sensitive to increases in the load level and appeared to approach an asymptotic limit. A least-squares fit to the finite element results indicated asymptotic values for θ_c of about 76 deg for $c_d = 1.6\%$ and about 83 deg for $c_d = 0.8\%$. In general, the $S_b - \theta_c$ curves in Fig. 6 show that the clearance had a strong influence on the contact angle.

The normalized hole boundary stresses are shown in Fig. 7 for the different values of c_d . All the results shown in this figure were calculated for a nominal bearing stress of 475 MPa. Again the dashed curves represent the snug-fit ($c_d = 0$) reference case, where $\theta_c = 83$ deg. For the case of $c_d = 0$, the peak value of $(\sigma_{\theta\theta}/S_b) = 1.16$ was reached about 2 deg beyond the contact region. The contact angle for the case of $c_d = 0.8\%$ was 65 deg. The peak value of $\sigma_{\theta\theta}/S_b$ here was 1.29, 11% higher than the snug-fit case. The contact angle for the 1.6% clearance case was only 53 deg. The peak value of $\sigma_{\theta\theta}/S_b$ was 1.34, which was about 16% higher than the snug-fit case. Furthermore, the peak value of σ_{rr}/S_b was 36% higher than that for the snug-fit case. Notice that for increasing clearance, the $\sigma_{\theta\theta}$ values decrease in the vicinity of $\theta = 0$. This trend can be explained by the decrease in θ_c . For very small θ_c values, the $\sigma_{\theta\theta}$ at $\theta = 0$ should approach that for a point load on a boundary and therefore would be compressive. In general, Fig. 7 shows that the peak stresses and their locations were strongly influenced by clearance.

For the $c_d = 0.8\%$, the radial (σ_{rr}) and tangential ($\sigma_{\theta\theta}$) stresses around the hole boundary are shown in Fig. 8 with several S_b levels. At each S_b level, the peak tangential stress occurs about 2 deg beyond the contact region. It is important to be able to determine the location of the peak value of $\sigma_{\theta\theta}$ because the onset of damage in composite joints may start at this location.¹⁴ Furthermore, under fatigue loading, the $\sigma_{\theta\theta}$ peak will move with the cyclic load which severely complicates the fatigue damage analyses.

The variations of the peak stresses with increasing stress level S_b are shown in Figs. 9 and 10 for several values of c_d . As expected, for the linear snug-fit case ($c_d = 0$), the peak $\sigma_{\theta\theta}$ and σ_{rr} stresses vary linearly with increasing S_b . For the clearance cases, both the peak $\sigma_{\theta\theta}$ stress and the peak σ_{rr} stress show a slight initial nonlinearity, although, at higher load levels, both peak stresses increase linearly. It is in-

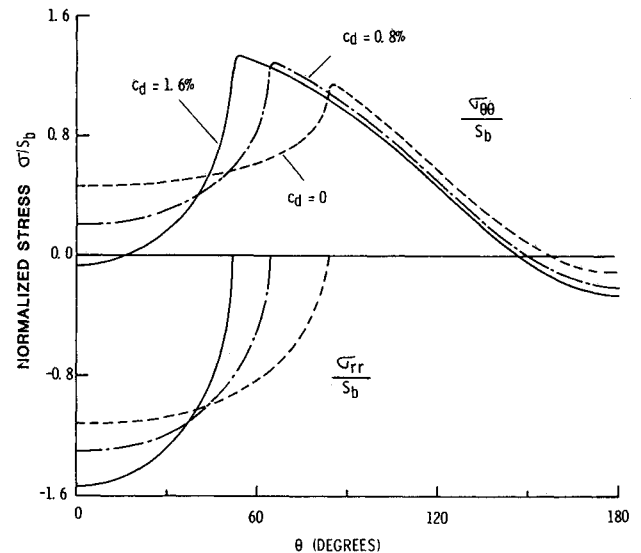


Fig. 7 Effect of clearance on local stresses.

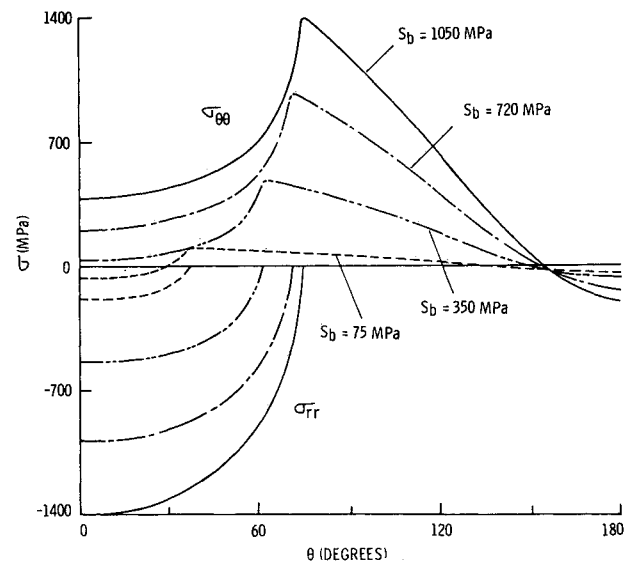


Fig. 8 Local stress distributions at different loads, $c_d = 0.8\%$.

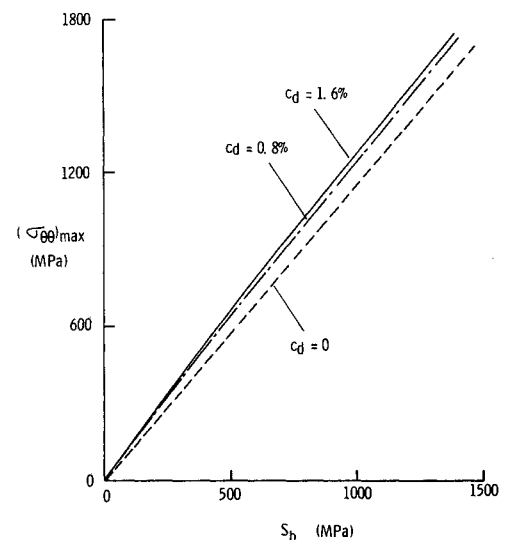


Fig. 9 Variation of peak tangential stress with S_b .

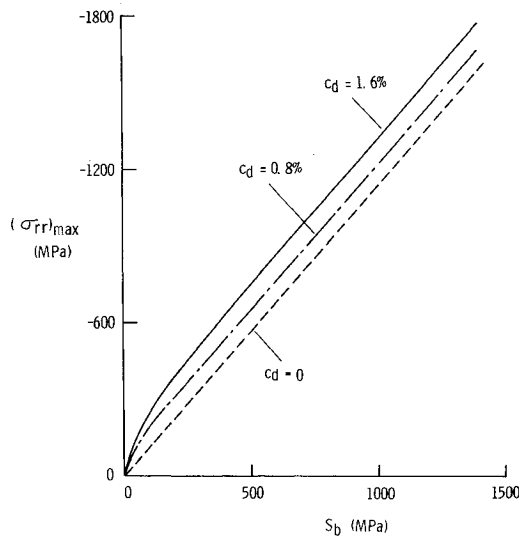


Fig. 10 Variation of peak radial stress with S_b .

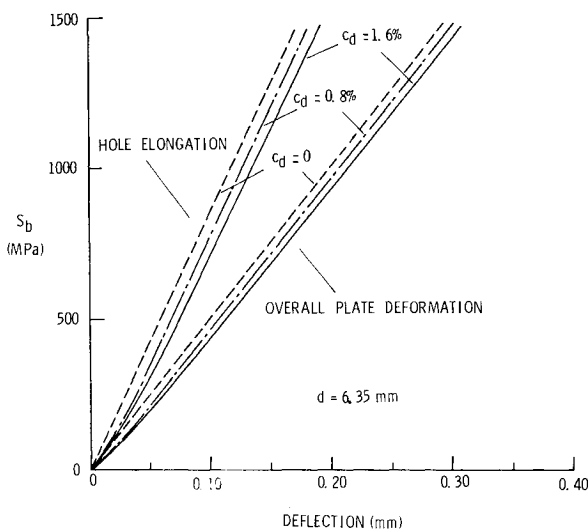


Fig. 11 Hole elongation and overall plate deformation.

interesting to note that, although the location of the peak $\sigma_{\theta\theta}$ stress changes nonlinearly with the load, the magnitude of the peak $\sigma_{\theta\theta}$ stress increases linearly after a slight initial nonlinearity.

Loading will cause the hole to elongate and the plate to deform. The hole elongation was calculated as the x -displacement of point D relative to fixed point A (see Fig. 3). The overall plate deformation was calculated as the x -displacement of the left end of the model. Figure 11 shows the change in the hole elongation and overall plate deformation with bearing stress for a 6.35 mm diameter hole. As expected for the snug-fit case, both the hole elongation and overall plate deformation vary linearly with increasing S_b . After a slight initial nonlinearity, the hole elongation and overall plate deformation also vary linearly with the increasing bearing stress for the clearance cases. At a typical laminate bearing strength level of $S_b = 1000$ MPa,¹⁴ the $c_d = 1.6\%$ case shows 16% higher hole elongation than for the snug-fitting case. As expected, when compared to the hole elongation, the overall plate deformation is less sensitive to clearance. Also the initial nonlinearity of the overall plate deformation is less severe. For the $c_d = 1.6\%$ case, overall plate deformation is only 7% higher than the reference $c_d = 0$ case at $S_b = 1000$ MPa. The length $L_t = 6d$ used in the present

study is typical of bolt spacing used in multifastener joints. Hence the above results for overall plate deformation suggest that clearance is probably not a critical factor in the stiffness analysis of multifastener joints.

Concluding Remarks

A simple method has been developed for the stress analysis of a clearance-fit bolt under bearing loads. This method uses a finite element analysis with an inverse formulation. Conditions along the bolt-hole interface are specified as displacement constraint equations. The present method is simple to apply and can be implemented with most general-purpose finite element programs. After the method was verified, by comparison with previous work, it was then applied to the analysis of a simple joint with a smooth, rigid, clearance-fit bolt. For values of diametrical clearance c_d typically used in composite joints, the effect of clearance on the contact angle, the local stresses, and joint stiffness were investigated.

The contact angle was found to be highly sensitive to changes in the clearance. Also the peak stresses and their locations were considerably influenced by the clearance. For example, when results for the $c_d = 1.6\%$ clearance case with a 475 MPa bearing stress were compared with the snug-fit case, the peak tangential stress was 16% higher, the peak radial stress was 36% higher, and the contact angle was about 30% smaller than for this reference case. After a slight initial nonlinearity, the peak stresses, the hole elongation, and the overall plate deformation in the clearance-fit joint increased linearly with increasing stress level. At a bearing stress S_b of 1000 MPa for $c_d = 1.6\%$, the hole elongation was 16% greater than for the $c_d = 0$ reference case; whereas, the overall plate deformation was only 7% greater than the $c_d = 0$ case. These results suggest that the clearance in a mechanically fastened joint should be considered in stress and strength analyses but may have little influence on joint stiffness.

References

- Harris, H. G., Ojalvo, I. U., and Hooson, R. E., "Stress and Deflection Analysis of Mechanically Fastened Joints," Grumman Aerospace Corp., Air Force Flight Dynamics Lab., Bethpage, New York, Rept. AFFDL-TR-70-49 (AD-709-221), May 1970.
- Oplinger, D. W. and Gandhi, K. R., "Analytical Studies of Structural Performance in Mechanically Fastened Fibre-Reinforced Plates," *Proceedings of the U.S. Army Symposium on Solid Mechanics*, 1974: *The Role of Mechanics in Design-Structural Joints*, Army Material and Mechanics Research Center, Watertown, MA, Rept. AMMRC MS 74-8 (AD 786 543), Sept. 1974, pp. 211-242.
- Waszczak, J. P. and Cruse, T. A., "Failure Mode and Strength Predictions of Anisotropic Bolt Bearing Specimens," *Journal of Composite Materials*, Vol. 5, July 1971, pp. 421-425.
- Eshwar, V. A., "Analysis of Clearance Fit Pin Joints," *International Journal of Mechanical Sciences*, Vol. 20, 1978, pp. 477-484.
- Mangalgiri, P. D., Dattaguru, B., and Rao, A. K., "Finite Element Analysis of Moving Contact in Mechanically Fastened Joints," *Nuclear Engineering and Design*, Vol. 78, 1984, pp. 303-311.
- Francavilla, A. and Zienkiewicz, O. C., "A Note on Numerical Computation of Elastic Contact Problems," *International Journal of Numerical Methods in Engineering*, Vol. 9, 1975, pp. 913-924.
- White, D. J. and Enderby, L. R., "Finite Element Stress Analysis of a Nonlinear Problem: A Connecting-Rod Eye Loaded by Means of a Pin," *Journal of Strain Analysis*, Vol. 5, No. 1, 1970, pp. 41-48.
- Sholes, A. and Strover, E. M., "The Piecewise-Linear Analysis of Two Connecting Structures Including the Effect of Clearance at the Connections," *International Journal of Numerical Methods in Engineering*, Vol. 3, 1971, pp. 45-51.

⁹Chan, S. K. and Tuba, I. S., "A Finite Element Method for Contact Problems of Solid Bodies—Part I. Theory and Validation," *International Journal of Mechanical Sciences*, Vol. 13, 1971, pp. 615-625.

¹⁰Rao, A. K., "Elastic Analysis of Pin Joints," *Computers and Structures*, Vol. 9, 1978, pp. 125-144.

¹¹Wilkinson, T. L., Rowlands, R. E., and Cook, R. D., "An Incremental Finite-Element Determination of Stresses Around Loaded Holes in Wood Plates," *Computers and Structures*, Vol. 14, No. 1-2, 1981, pp. 123-128.

¹²Kim, W., "Stress Analysis Methods for Clearance-Fit Mechanical Joints in Laminated Composites," Ph.D. Thesis, Rensselaer Polytechnic Institute, Troy, NY, 1982.

¹³DOD/NASA Advanced Composites Design Guide, Vol. IV-A: Materials, First Edition, Contract F33615-78-C-3203, Air Force Wright Aeronautical Laboratories, July 1983, (available as NASA CR-173407 and from DTIC as AD B080 184L).

¹⁴Crews, J. H., Jr. and Naik, R.V.A., "Failure Analysis of a Graphite/Epoxy Laminate Subjected to Bolt Bearing Loads," NASA TM 86297, Aug. 1984.

From the AIAA Progress in Astronautics and Aeronautics Series . . .

COMBUSTION EXPERIMENTS IN A ZERO-GRAVITY LABORATORY—v. 73

Edited by Thomas H. Cochran, NASA Lewis Research Center

Scientists throughout the world are eagerly awaiting the new opportunities for scientific research that will be available with the advent of the U.S. Space Shuttle. One of the many types of payloads envisioned for placement in earth orbit is a space laboratory which would be carried into space by the Orbiter and equipped for carrying out selected scientific experiments. Testing would be conducted by trained scientist-astronauts on board in cooperation with research scientists on the ground who would have conceived and planned the experiments. The U.S. National Aeronautics and Space Administration (NASA) plans to invite the scientific community on a broad national and international scale to participate in utilizing Spacelab for scientific research. Described in this volume are some of the basic experiments in combustion which are being considered for eventual study in Spacelab. Similar initial planning is underway under NASA sponsorship in other fields—fluid mechanics, materials science, large structures, etc. It is the intention of AIAA, in publishing this volume on combustion-in-zero-gravity, to stimulate, by illustrative example, new thought on kinds of basic experiments which might be usefully performed in the unique environment to be provided by Spacelab, i.e., long-term zero gravity, unimpeded solar radiation, ultra-high vacuum, fast pump-out rates, intense far-ultraviolet radiation, very clear optical conditions, unlimited outside dimensions, etc. It is our hope that the volume will be studied by potential investigators in many fields, not only combustion science, to see what new ideas may emerge in both fundamental and applied science, and to take advantage of the new laboratory possibilities.

Published in 1981, 280 pp., 6×9, illus., \$25.00 Mem., \$39.00 List

TO ORDER WRITE: Publications Order Dept., AIAA, 1633 Broadway, New York, N.Y. 10019